JAERI-M
92-083

MEASUREMENTS OF BREAKAWAY REACTION BETWEEN BERYLLIUM AND WATER VAPOR FOR ITER BLANKET DESIGN

June 1992

Hiroshi YOSHIDA, Kusuo ASHIBE*, Kiyoshi ONO*
and Mikio ENOEDA

日本原子力研究所
Japan Atomic Energy Research Institute

JAERI-Mレポートは，日本原子力研究所が不定期に公刊している研究報告書です。
入手の問合わせは，日本原子力研究所技術情報部情報資料課（〒319-11茨城県那珂郡東海村）あて，お申しこしください。なお，このほかに財団法人原子力弘済会資料センター（〒319-11 茨城県那珂郡東海村日本原子力研究所内）で複写による実費領布をおこなっております。

JAERI-M reports are issued irregularly.
Inquiries about availability of the reports should be addressed to Information Division, Department of Technical Information, Japan Atomic Energy Research Institute, Tokai-mura, Naka-gun, Ibaraki-ken 319-11, Japan.

編集兼発行　日本原子力研究所
印　　刷　㈱原子力資料サービス

JAERI-M 92-083

Measurements of Breakaway Reaction Between Beryllium and Water Vapor for ITER Blanket Design

Hiroshi YOSHIDA, Kusuo ASHIBE*, Kiyoshi ONO*
and Mikio ENOEDA

Department of Fusion Engineering Research
Naka Fusion Research Establishment
Japan Atomic Energy Research Institute
Naka-machi, Naka-gun, Ibaraki-ken

(Received May 14, 1992)

Beryllium will be utilized as the neutron multiplier in the ITER breeding blanket. As part of Japanese contribution of the water-cooled blanket design, preliminary study was performed to investigate beryllium breakaway reaction, which is one of safety issues of ITER under high temperature conditions.

Thermogravimetric measurements in the temperature range 550 - 750 °C were carried out under helium gas flow containing water vapor of 7.6 and 0.76 Torr. The test samples were prepared from commertially available hot-pressed & hot-rolled beryllium plates. Characterization of the surface reaction product was performed by macro and microscopic observations, and X-ray diffraction analysis.

Linear and parabolic rate laws were found for the dominant reaction steps in the preceding period of the breakaway reaction. Microstructure of the surface reaction layer formed in all exposure conditions revealed brittle structure, which was composed of blister and microcracks. The following rate equations were obtained for the preceding step of breakaway reaction.

(i) In case of 750 °C - 7.6 Torr

$W(mg/cm^2) = k \cdot t(min)$

---

* Toshiba Corporation

JAERI－M 92－083

ITERブランケットを対象としたベリリウム－水蒸気系の高温反応実験

日本原子力研究所那珂研究所核融合工学部
吉田　浩・芦部　楠夫*・小野　清*
榎枝　幹男

（1992年5月14日受理）

ITERブランケットの設計基準に選定された水冷却・固体増殖材ブランケットでは，冷却水が漏洩した際に中性子増倍材（ベリリウム）と水蒸気との反応でH_2ガス及び有毒なBeO粉塵が生成する可能性が高い。

本実験は，Be－H_2O系の高温反応を定量的に把握し，今後のブランケット設計に反映することを目的として実施したものである。実験では，ブランケット内の温度分布及び小数の冷却管破損を想定し，温度550～750℃，水蒸気分圧0.76～7.6 Torrを選定した。ベリリウムは，代表的な製法（ホットプレス熱間圧延）による金属板を用いた。

本実験により，550℃以上の温度では一定の誘導期間を経て加速度的酸化（breakaway reaction）が起こること，誘導期間は材料の表面状態にあまり依存せず750℃，650℃，600℃でそれぞれ0.3～5時間，10～20時間，40～70時間であることが分かった。誘導期間における主反応の速度式として次の実験式を得た。

(i) 750℃，7.6 Torr－H_2Oの場合

$$W\ (mg \cdot cm^{-2}) = k \cdot t\ (min)$$

$$k\ (mg \cdot cm^{-2} \cdot min^{-1}) = (1.8 \sim 7.0) \times 10^{-4}$$

(ii) 650℃，0.76 Torr－H_2Oの場合

$$W\ (mg \cdot cm^{-2}) = k \cdot t^{1/2}\ (min)^{1/2}$$

$$k\ (mg \cdot cm^{-2} \cdot min^{-1/2}) = (7.7 \sim 9.0) \times 10^{-4}$$

ここに，dW，k，tは，それぞれ重量変化，速度定数及び時間である。

那珂研究所：〒311－01　茨城県那珂郡那珂町大字向山801－1
＊㈱東芝

Contents

目　　次

1. Introduction

Development of blanket with tritium breeding ratio (TBR) greater than unity is essential for the realization of fusion energy reactor. Preliminary work on breeding blanket was carried out to support design work of ITER driver blanket in the phase of conceptual design activity (CDA). Water-cooled ceramic breeder blanket was selected as the design reference by the end of the CDA [1]. All concepts of the blanket proposed by four parties of ITER participants utilize lithium ceramic (tritium breeder), beryllium (neutron multiplier) and SS316 (structure material). Allowable material temperatures will dominate the design configuration of each concept. Both concepts of Japan and USA employ beryllium layers as the temperature control media between water coolant (60 - 100 °C) and breeder (450 - 1000 °C). The design temperature of beryllium currently determined to be about 500 °C [2] . As one of safety issues in ITER blanket design, it is noticed that there is a possibility of beryllium combustion at accidental situations such as coolant leakage and air leakage [3].

Beryllium is a very stable metal in the atmosphere, because it forms a protective oxide film on the surface of metal at moderate temperature less than 100 C. Meanwhile at high temperatures, it severely reacts with various gases such as O_2, N_2, CO, CO_2 and water vapor [4,5,6]. The beryllium breakaway reaction, in which reaction rate is highly accelerated with elapsed time, with water vapor has also been studied by Aylmore [7], Sasabe [8], and Blumenthal [9]. The reaction in the beryllium-water vapor system is expressed by the following reaction fomula; $Be(s) + H_2O(g) \rightarrow BeO(s) + H_2(g) + 608.4$ kJ/mol. Therefore, the breakaway phenomena will be characterized by rapid formation of hydrogen gas and hazardous dust of beryllium oxide as well as large heat generation (it is greater than that of hydrogen-oxygen reaction by 2.5 times).

Current Japanese blanket concept (Fig. 1) is composed of packed beds of beryllium pebble (diameter: 1-6 mm), so that the effective surface area of beryllium in the packed beds is extreamely large. From safety aspect of water-cooled blanket for ITER, it is necessary to evaluate the impact of internal water leakage (from coolant panel to beryllium zone and breeder zone). Present study was planned to obtain basic data of high temperature beryllium-water vapor reaction assuming

small amount of water leakage into the beryllium zone.

2. Experimental Procedure

2.1 Experimental apparatus

A thermogravimetric measurement system (Fig. 2) was fabricated. It is composed of a microbalance with an electric furnace (Fig. 3), helium purge gas system with humidifier, and vacuum pumping system. The microbalance (CAHN-C2000 with maximum sensitivity of 0.1 μg) was put on a special vibration proof bench, and placed in a small room equipped with temperature control devices. Temperature variation around the microbalance could be kept within ±0.1 °C. Pressure and flow rate of helium-water vapor mixture were adjusted with pressure gauges (Ba), mass flow controllers (MFC) and hygrometers (M1,M2). Temperatures of test samples were measured with thermocouples attached near the beryllium sample and the internal wall of the test section of microbalance, which is assembled with quartz tube (diameter: 35 mm - OD).

2.2 Preparation of Test Samples

Test samples were obtained from two different companies (NGK: Japan, Brush Wellmann: USA). All samples were prepared from hot-pressed and hot-rolled beryllium plates. The following are their specifications;

(i) NGK samples

Dimensions: 20 mm × 10 mm × 1 mm

Surface treatment:

BR-3 : As received (mechanically ground)

BR-3E : As received (chemically polished and cut)

BR-3EE : Chemically polished BR-3

Composition of BR-3 (Lot No. 4310):

BeO	1.00 wt.%	C	0.09 wt.%
Fe	0.09	Si	0.03
Al	0.04	Others	< 0.04
Mg	0.01		

(ii) Brush Wellmann samples

Dimensions: 20 mm × 10 mm × 1 mm

Surface treatment:

PF-60 : As received (mechanically ground)

small amount of water leakage into the beryllium zone.

2. Experimental Procedure

2.1 Experimental apparatus

A thermogravimetric measurement system (Fig. 2) was fabricated. It is composed of a microbalance with an electric furnace (Fig. 3), helium purge gas system with humidifier, and vacuum pumping system. The microbalance (CAHN-C2000 with maximum sensitivity of 0.1 μg) was put on a special vibration proof bench, and placed in a small room equipped with temperature control devices. Temperature variation around the microbalance could be kept within ±0.1 °C. Pressure and flow rate of helium-water vapor mixture were adjusted with pressure gauges (Ba), mass flow controllers (MFC) and hygrometers (M1,M2). Temperatures of test samples were measured with thermocouples attached near the beryllium sample and the internal wall of the test section of microbalance, which is assembled with quartz tube (diameter: 35 mm - OD).

2.2 Preparation of Test Samples

Test samples were obtained from two different companies (NGK: Japan, Brush Wellmann: USA). All samples were prepared from hot-pressed and hot-rolled beryllium plates. The following are their specifications;

(i) NGK samples

Dimensions: 20 mm × 10 mm × 1 mm

Surface treatment:

BR-3 : As received (mechanically ground)

BR-3E : As received (chemically polished and cut)

BR-3EE : Chemically polished BR-3

Composition of BR-3 (Lot No. 4310):

BeO	1.00 wt.%	C	0.09 wt.%
Fe	0.09	Si	0.03
Al	0.04	Others <	0.04
Mg	0.01		

(ii) Brush Wellmann samples

Dimensions: 20 mm × 10 mm × 1 mm

Surface treatment:

PF-60 : As received (mechanically ground)

PF-60EE : Chemically polished

SR-200 : As received (mechanically ground)

Composition:

PF-60 (Lot No.3773B)		SR-200 (Lot No.3107B)	
Be	99.1 wt.%	Be	99.1 wt.%
BeO	0.7	BeO	1.0
Fe	0.05	Fe	0.06
C	0.04	C	0.12
Al	<0.01	Al	0.03
Mg	<0.001	Mg	<0.01
N	<0.01	Si	0.02
Mn	0.001	Others	<0.04
Cr	<0.01	(metallic elements)	
Ni	<0.01		
Co	<0.01		
Li	<0.003		
B	<0.002		

(iii) Chemical polishing

In order to make smooth the surface of beryllium, samples of BR-3E, BR-3EE and PF-60EE were chemically polished by the following conditions;

Solution : Mixture of 5 vol.%-Sulfuric acid and 95 vol.%-Phosphoric acid

Temperature : 100 °C

Exposure time : 20 - 50 s

2.3 Surface characteristics of test samples

Figs. 4(a)-(f) show difference in the surfaces of as received and chemically polished samples of BR-3, PF-60 and SR-200.

Figs. 5(a)-(f) of SEM photographs show surface characteristics of BR-3 (as received), BR-3E (as received and BR-3EE (chemically polished). Sharp scratches caused by mechanical grinding were observed on the surfaces of flat and edge areas of BR-3. The smooth surface of BR-3E is the feature of chemically polished samples. The similar characteristics can be seen on the surfaces of BR-3EE (Fig. 5(e),(f)). The surface similarity among PF-60 and SR-200 is also observed (Figs. 6(a)-(d)), however both reveal a lot of small pores caused by mechanical grinding.

2.4 Test Conditions

Thermogravinmetric measurements were carried out under differnt temperatures (550 °C, 600 °C, 650 °C and 750 °C) and water vapor pressures (7.6 Torr and 0.76 Torr). The experimental conditions were summarized in Table 1.

3. Results and Discussion

3.1 Kinetic measurements

Fig. 7 shows all results of weight gain during exposure with water vapor. Apparent breakaway reaction is observed for all types of samples at temperatures higher than 600 °C. Clear tendency toward the breakaway in the conditoins of 550 °C (Run-14) and of 0.76 Torr (Run-7) was not observed in the present exposure duration. Reproduciability (within factors 2 - 3) in the time dependence of breakaway reaction at 650 °C (Runs-10, 11) and 600 °C (Runs-9, 12) was confirmed with samples of BR-3EE. Meanwhile, effects of surface treatments and type of samples on the breakaway time are not clear. For example, from comparison of the breakaway time among as received samples (Run-4: PF-60, Run-3: BR-3 and Run-5: SR-200), SR-200 seems less reactive than the others. This reactivity does not consistent with surface roughness of as received samples (roughness of SR-200 seems greater than that of PF-60 and BR-3). For chemically polished samples of BR-3EE, a correlation between the preceding time for the start of breakaway and exposure temperature was found.

Figs. 8-11 are the Log-Log plot of the weight gain in the derivative period. The n values determened for each reaction step represent type of rate equation.

Fig. 8, shows temperature effect on the early stage of reaction with vapor pressure of 7.6 Torr at 750 °C and 650 °C. For 750 °C (Run-1), linear rate reaction, which is expressed by slope = 1.0, occurred immediately after start of exposure, and it is dominant until initiation of the breakaway. The reaction of the intermediate step was expressed by slope = 1.4. Higher power rate reaction due to a complex interactions of blister formation and hydrogen effects have been reported by Sasabe [8], however mechanism of this step was not clear in the present experiment. In case of 650 °C (Run-2), three steps seems to be appeared in the derivative period. Mechanism for the steps of slop = 0.61 and 0.34 can not also be explained, but it seems that parabolic rate reaction

2.4 Test Conditions

Thermogravinmetric measurements were carried out under differnt temperatures (550 °C, 600 °C, 650 °C and 750 °C) and water vapor pressures (7.6 Torr and 0.76 Torr). The experimental conditions were summarized in Table 1.

3. Results and Discussion

3.1 Kinetic measurements

Fig. 7 shows all results of weight gain during exposure with water vapor. Apparent breakaway reaction is observed for all types of samples at temperatures higher than 600 °C. Clear tendency toward the breakaway in the conditoins of 550 °C (Run-14) and of 0.76 Torr (Run-7) was not observed in the present exposure duration. Reproduciability (within factors 2 - 3) in the time dependence of breakaway reaction at 650 °C (Runs-10, 11) and 600 °C (Runs-9, 12) was confirmed with samples of BR-3EE. Meanwhile, effects of surface treatments and type of samples on the breakaway time are not clear. For example, from comparison of the breakaway time among as received samples (Run-4: PF-60, Run-3: BR-3 and Run-5: SR-200), SR-200 seems less reactive than the others. This reactivity does not consistent with surface roughness of as received samples (roughness of SR-200 seems greater than that of PF-60 and BR-3). For chemically polished samples of BR-3EE, a correlation between the preceding time for the start of breakaway and exposure temperature was found.

Figs. 8-11 are the Log-Log plot of the weight gain in the derivative period. The n values determened for each reaction step represent type of rate equation.

Fig. 8, shows temperature effect on the early stage of reaction with vapor pressure of 7.6 Torr at 750 °C and 650 °C. For 750 °C (Run-1), linear rate reaction, which is expressed by slope = 1.0, occurred immediately after start of exposure, and it is dominant until initiation of the breakaway. The reaction of the intermediate step was expressed by slope = 1.4. Higher power rate reaction due to a complex interactions of blister formation and hydrogen effects have been reported by Sasabe [8], however mechanism of this step was not clear in the present experiment. In case of 650 °C (Run-2), three steps seems to be appeared in the derivative period. Mechanism for the steps of slop = 0.61 and 0.34 can not also be explained, but it seems that parabolic rate reaction

expressed by slope = 0.5 dominates the preceding period. On the contrary, in Fig. 9, the linear rate law is apparently held for different samples. The reaction rate of BR-3E is larger than that of PF-60 by factors.

Fig. 10 shows good reproduciability among three tests (Runs-3, 10 and 11) with two different samples (BR-3E and BR-3EE). Parabolic rate law is held from early stage through the start of breakaway.

Fig. 11 shows reaction characteristics for the low vapor pressure of 0.76 Torr. It also indicates that parabolic rate law is dominant.

Based on these experimental results, it was found that major reaction rate equations can be expressed by the following formula.

$W = k \cdot t^n$

W : weight gain (mg/cm^2)

t : time (min)

k : rate constant ($mg/cm^2/min^{-n}$).

From Table 2, which summarizes rate constants for all Runs, it can be concluded that the breakaway occurres even if parabolic oxidation is dominant in the preceding reaction step. That is, the oxide layer formed at temperatures higher than 600 °C is not protective. It should be noticed that accelerative reaction observed in the present work can only be explained by considering rapid increase of effective surface area of beryllium substrate. Such increase may be resulted from fructure of surface microstructure of beryllium substrate. Several mechanisms such as void formation due to migration of Be atom from substrate to outside of oxide layer, blister formation by hydrogen gas precipitation, etch-pit formation based on dislocation and microcrack generation due to difference of molar volume between BeO (8.3 cm^3/mol) and Be (4.9 cm^3/mol) can attribute to such brittle failure of beryllium metal.

3.2 Analysis of reaction product

Figs. 12(a), (b) show typical macroscopic appearance after breakaway reaction at 750 °C (Run-3: BR-3, vapor pressure = 7.6 Torr, exposure time = 2.5 h). The entire surface was covered with fine powder of reaction product (dark gray). Severe reaction occurred at edges of sample. The localized severe reaction may be caused by either stress concentration resulted from the molar volume change in accorance with BeO formation or local residual stress generated in sample preparation.

Fig. 13, X-ray diffraction pattern of powder removed from this sample surface, indicates that the reaction product is a mixture of beryllium oxide and small of beryllium metal. This fact proves the sutface fractuation of beryllium metal, which is expected to occure during breakaway reaction.

3.3 Microscopic observations

After completion of weight gain measurement, surface of typical samples was investigated by SEM observation.

(i) Surface characteristics for the exposure at 750 °C (Run-1: BR-3E, 7.6 Torr)

Figs. 14(a)-(c) show the surface exposed to water vapor of 7.6 Torr at 750 °C for 9.9 h. The microstructure shown in Fig. 14(b) is composed of blister and large ckacks. It was typical feature of reaction product at the flat part of test samples. Some of the blisters reveal teared-up feature indicating burst of blisters. This fact may be a evidence of that part of hydrogen gas formed by the following reaction was accumulated in the layer of beryllium oxide;

$$Be(s) + H_2O \rightarrow BeO + H_2(g)$$

On the contrary, as shown in Fig. 14(c), surface of the reaction layer at the edge part is composed of particles (average size: 15 μm) and blisters. This fact proves that edge part of the sample is more active than flat area.

Figs. 15(a)-(c), cross-sectional view of sample of Run-1, show that surface of beryllium metal substrate was severly attacked and formed brittle texture in the reaction zone. This structural feature is proved by the X-ray diffraction analysis indicating the reaction zone contains Be (Fig. 13).

(ii) Material comparison with as-received samples of mechanically ground (Run-3: BR-3, Run-4: PF-60, Run-5: SR-200)

Figs. 16(a)-(f) show typical surface microstructure of the mechanically ground samples after breakaway measurement at 750 °C with vapor pressure of 7.6 Torr. Particles precipitated on the surface of reaction layer was previously removed by ultrasonic solvent cleaning. The

surface reaction layer formed on each sample seems weak scale composed of blisters and microcracks. Especially, Fig. 16(f) shows both the blisters and the original scratch feature of the sample (see Figs. 6(c), (d)).

(iii) Effect of water vapor pressure (Run-6: BR-3E, 750 °C, 0.76 Torr)

In this experiment, exposure (for 16.3 h) was stopped before the start of breakaway reaction. As shown in Figs. 17(a),(b), however, the microstructure presents almost same features as that of higher vapor pressure (7.6 Torr) tests (see Fig. 14(b), Fig. 16(c), (d), and Figs. 16(e),(f)). Therefore, it can be said that the breakaway reaction will be generated even at low vapor pressure, and that its breakaway time will depend on the pressure.

(iv) Surface characteristics for the exposure at 550 °C (Run-14: BR-3EE, 7.6 Torr)

Rapid weight change by the breakaway reaction was not observed, and the surface of sample slightly lost its original luster. However as shown in Figs. 18(a)-(d), its reaction layer shows microcracks, blisters and grain-boundary attack. These are the feature of the previous tests at higher temperatures, so that it is assumed that the breakaway can be induced even at 550 °C. The breakaway time is estimated to be 600 - 1000 h from experimental correlation shown in Fig. 19.

4. Summary

In order to examine kinetics of the breakaway reaction between beryllium and water vapor at high temperature, thermo-gravimetric measurement, microscopic observation and X-ray diffraction analysis were carried out. Test samples were prepared from commertial beryllium plate produced by hot-press and hot-roll. Experimental conditions of temperature and vapor pressure were determined to simulate small water leakage in beryllium packed bed of ITER blanket.

The following are the major results of this study.

(a) Breakaway reaction occurred at 750 °C, 650 °C and 600 °C with vapor pressure of 7.6 Torr.

(b) Breakaway reaction did not occurred in the present exposure conditions of 550 °C - 7.6 Torr - 595.5 h and 750 °C - 0.76 Torr - 16.3

surface reaction layer formed on each sample seems weak scale composed of blisters and microcracks. Especially, Fig. 16(f) shows both the blisters and the original scratch feature of the sample (see Figs. 6(c), (d)).

(iii) Effect of water vapor pressure (Run-6: BR-3E, 750 °C, 0.76 Torr)

In this experiment, exposure (for 16.3 h) was stopped before the start of breakaway reaction. As shown in Figs. 17(a),(b), however, the microstructure presents almost same features as that of higher vapor pressure (7.6 Torr) tests (see Fig. 14(b), Fig. 16(c), (d), and Figs. 16(e),(f)). Therefore, it can be said that the breakaway reaction will be generated even at low vapor pressure, and that its breakaway time will depend on the pressure.

(iv) Surface characteristics for the exposure at 550 °C (Run-14: BR-3EE, 7.6 Torr)

Rapid weight change by the breakaway reaction was not observed, and the surface of sample slightly lost its original luster. However as shown in Figs. 18(a)-(d), its reaction layer shows microcracks, blisters and grain-boundary attack. These are the feature of the previous tests at higher temperatures, so that it is assumed that the breakaway can be induced even at 550 °C. The breakaway time is estimated to be 600 - 1000 h from experimental correlation shown in Fig. 19.

4. Summary

In order to examine kinetics of the breakaway reaction between beryllium and water vapor at high temperature, thermo-gravimetric measurement, microscopic observation and X-ray diffraction analysis were carried out. Test samples were prepared from commertial beryllium plate produced by hot-press and hot-roll. Experimental conditions of temperature and vapor pressure were determined to simulate small water leakage in beryllium packed bed of ITER blanket.

The following are the major results of this study.

(a) Breakaway reaction occurred at 750 °C, 650 °C and 600 °C with vapor pressure of 7.6 Torr.

(b) Breakaway reaction did not occurred in the present exposure conditions of 550 °C - 7.6 Torr - 595.5 h and 750 °C - 0.76 Torr - 16.3

h. However, surface microstructure of the reaction layers in each sample indicated that the breakaway will eventually be induced.

(c) The preceding reaction steps for initiation of the breakaway mainly depended on temperature and vapor pressure.

(d) The major reactions in the preceding steps were dominated by linear rate law and/or parabolic rate law, and the rate equations were determined in all exposure tests.

(e) A correlation between the breakaway time and temperature was found.

(f) Powder X-ray diffraction analysis proved that reaction procuct is composed of BeO and small amount of Be metal.

(g) Micro and mocroscopic observations revealed that surface reaction product is composed of fine particles of BeO and brittle reaction layer, which included various defects such as blisters and micro-cracks.

Acknowledgement

The authors wish to thank Mr. Y. Naruse, chief of Tritium Engineering Laboratory. Tokai, JAERI, and Dr. S. Kobayashi, manager of Fusion Technology Development, Toshiba Corp. for their heartiful encouragement on the present work.

References

1) ITER Blanket and Shield Conceptual Design, and ITER Material Evaluation and Data Base, ITER Documentation Series, No.29, IAEA. Vienna 1991

2) T. Kuroda et al., Japanese Contributions to Blanket Design for ITER, JAERI-M 91-133(1991)

3) S.J. Piet, Safety and Environmental challenges in Materials Selection, J. Nucl. Mater., 141-143, 65(1986)

4) Gmelin Handbook of Inorganic Chemistry: Beryllium, 8th edition, Supplement Volume A1, Chapter 6, SPRINGLER-VERLAG BERLIN/HELDELBERG/ NEW YORK/TOKYO (1986)

5) G. Ervin, Jr, and T.L. Mackay, Catastrophic Oxidation of Beryllium Metal, J. of Nucl. Maters., 12(1), 30 (1963)

6) W.J. Werner, et al., The Reactions of Beryllium with Wet Carbon Oxide, The Metallurgy of Beryllium, THE INSTITUTE OF METALS, LONDON, 283-294 (1963)

h. However, surface microstructure of the reaction layers in each sample indicated that the breakaway will eventually be induced.

(c) The preceding reaction steps for initiation of the breakaway mainly depended on temperature and vapor pressure.

(d) The major reactions in the preceding steps were dominated by linear rate law and/or parabolic rate law, and the rate equations were determined in all exposure tests.

(e) A correlation between the breakaway time and temperature was found.

(f) Powder X-ray diffraction analysis proved that reaction procuct is composed of BeO and small amount of Be metal.

(g) Micro and mocroscopic observations revealed that surface reaction product is composed of fine particles of BeO and brittle reaction layer, which included various defects such as blisters and micro-cracks.

Acknowledgement

The authors wish to thank Mr. Y. Naruse, chief of Tritium Engineering Laboratory. Tokai, JAERI, and Dr. S. Kobayashi, manager of Fusion Technology Development, Toshiba Corp. for their heartiful encouragement on the present work.

References

1) ITER Blanket and Shield Conceptual Design, and ITER Material Evaluation and Data Base, ITER Documentation Series, No.29, IAEA. Vienna 1991

2) T. Kuroda et al., Japanese Contributions to Blanket Design for ITER, JAERI-M 91-133(1991)

3) S.J. Piet, Safety and Environmental challenges in Materials Selection, J. Nucl. Mater., 141-143, 65(1986)

4) Gmelin Handbook of Inorganic Chemistry: Beryllium, 8th edition, Supplement Volume A1, Chapter 6, SPRINGLER-VERLAG BERLIN/HELDELBERG/ NEW YORK/TOKYO (1986)

5) G. Ervin, Jr, and T.L. Mackay, Catastrophic Oxidation of Beryllium Metal, J. of Nucl. Maters., 12(1), 30 (1963)

6) W.J. Werner, et al., The Reactions of Beryllium with Wet Carbon Oxide, The Metallurgy of Beryllium, THE INSTITUTE OF METALS, LONDON, 283-294 (1963)

h. However, surface microstructure of the reaction layers in each sample indicated that the breakaway will eventually be induced.

(c) The preceding reaction steps for initiation of the breakaway mainly depended on temperature and vapor pressure.

(d) The major reactions in the preceding steps were dominated by linear rate law and/or parabolic rate law, and the rate equations were determined in all exposure tests.

(e) A correlation between the breakaway time and temperature was found.

(f) Powder X-ray diffraction analysis proved that reaction procuct is composed of BeO and small amount of Be metal.

(g) Micro and mocroscopic observations revealed that surface reaction product is composed of fine particles of BeO and brittle reaction layer, which included various defects such as blisters and micro-cracks.

Acknowledgement

The authors wish to thank Mr. Y. Naruse, chief of Tritium Engineering Laboratory. Tokai, JAERI, and Dr. S. Kobayashi, manager of Fusion Technology Development, Toshiba Corp. for their heartiful encouragement on the present work.

References

1) ITER Blanket and Shield Conceptual Design, and ITER Material Evaluation and Data Base, ITER Documentation Series, No.29, IAEA. Vienna 1991

2) T. Kuroda et al., Japanese Contributions to Blanket Design for ITER, JAERI-M 91-133(1991)

3) S.J. Piet, Safety and Environmental challenges in Materials Selection, J. Nucl. Mater., 141-143, 65(1986)

4) Gmelin Handbook of Inorganic Chemistry: Beryllium, 8th edition, Supplement Volume A1, Chapter 6, SPRINGLER-VERLAG BERLIN/HELDELBERG/ NEW YORK/TOKYO (1986)

5) G. Ervin, Jr, and T.L. Mackay, Catastrophic Oxidation of Beryllium Metal, J. of Nucl. Maters., 12(1), 30 (1963)

6) W.J. Werner, et al., The Reactions of Beryllium with Wet Carbon Oxide, The Metallurgy of Beryllium, THE INSTITUTE OF METALS, LONDON, 283-294 (1963)

7) D.W. Aylmore et al., The high Temperature Oxidation of Beryllium, Par IV: In Water Vapor and in Moist Oxygen, J. of Nucl. Mater., 3(2), 190-200 (161)
8) M. Sasabe et al., Nippon Genshiryoku Gakkaishi, 10(6), 319 (1968)
9) J.L. Blumenthal et al., Proc. of 11th Symp. Intern. Combust., 417/25 (1966/67)

Table 1 Summary list of experimental conditions

Run No.	Samples	Temperature*1 (℃)	Exposure time(h)	He flow rate*2 (cm^3-STP/min)	Moisture level(Torr)	
					Inlet	Outlet*3
1	BR-3E	750/754	9.9	10/10	7.6	2.3/4.6
2	BR-3E	650/655	17.0	20/20	7.6	3.0/5.3
3	BR-3	749/760	2.5	20/20	7.6	3.8/4.6
4	PF-60	750/750	1.1	20/20	7.6	3.0/4.6
5	SR-200	750/764	5.3	20/20	7.6	3.0/5.3
6	BR-3E	759/763	16.3	10/90	0.76	0.4/0.6
7	BR-3EE	-/752	5.5	20/20	7.6	4.6/5.3
8	PF-60EE	-/751	1.7	20/20	7.6	4.6/5.3
9	BR-3EE	-/500	141.6	20/20	7.6	4.6/6.1
10	BR-3EE	-/650	27.5	20/-	7.6	1.5/6.8
11	BR-3EE	-/650	46.0	40/-	7.6	6.1/8.4
12	BR-3EE	-/600	158.0	40/-	7.6	7.6/8.4
13	BR-3EE	-/550	5.5	40/-	7.6	7.6/6.8
14	BR-3EE	-/550	595.5	40/-	7.6	6.8/8.4

*1 top/bottom: gas temperature/inner wall temperature
*2 top/bottom: fumidified He flow/dry He flow
*3 top/bottom: initial level/end level

Table 2 Rate constants of derivative period for breakaway reaction

Sample	Run No.	Temperature*1 (℃)	Moisture (Torr)	Time interval (min)	n (-)	k ($mg \cdot cm^{-2} \cdot min^{-n}$)
BR-3	3	750	7.6	1 - 4 4 - 20 20 - 90 90 - 150	1.0 1.4 1.0 AC	3.1E-4 1.6E-4 5.6E-4
BR-3E	1	750	7.6	4 - 200 200 - 600	1.0 AC	2.6E-4
	6	750	0.76	1 - 6 6 - 30 30 - 500 500 - 1000	0.5 1.0 0.5 0.6	4.3E-4 2.2E-4 9.8E-4 3.7E-4
	2	650	7.6	2 - 100 100 - 360 360 - 1000	0.6 0.3 0.5	5.9E-4 2.0E-3 7.8E-4
PF-60	4	750	7.6	2 - 20 20 - 70	1.0 AC	7.0E-4
PF-60E	8	750	7.6	5 - 20 20 - 100	1.0 AC	4.3E-4
SR-200	5	750	7.6	1 - 30 30 - 230	0.4 1.0	7.9E-4 1.1E-4
BR-3EE	7	750	7.6	3 - 10 10 - 100 100 - 350	1.0 0.3 AC	1.5E-3 1.0E-2
	10	650	7.6	4 - 480 480 - 2760	0.5 AC	2.6E-4
	11	650	7.6	1 - 900 900 - 1650	0.5 AC	2.6E-4

AC: Breakaway reaction

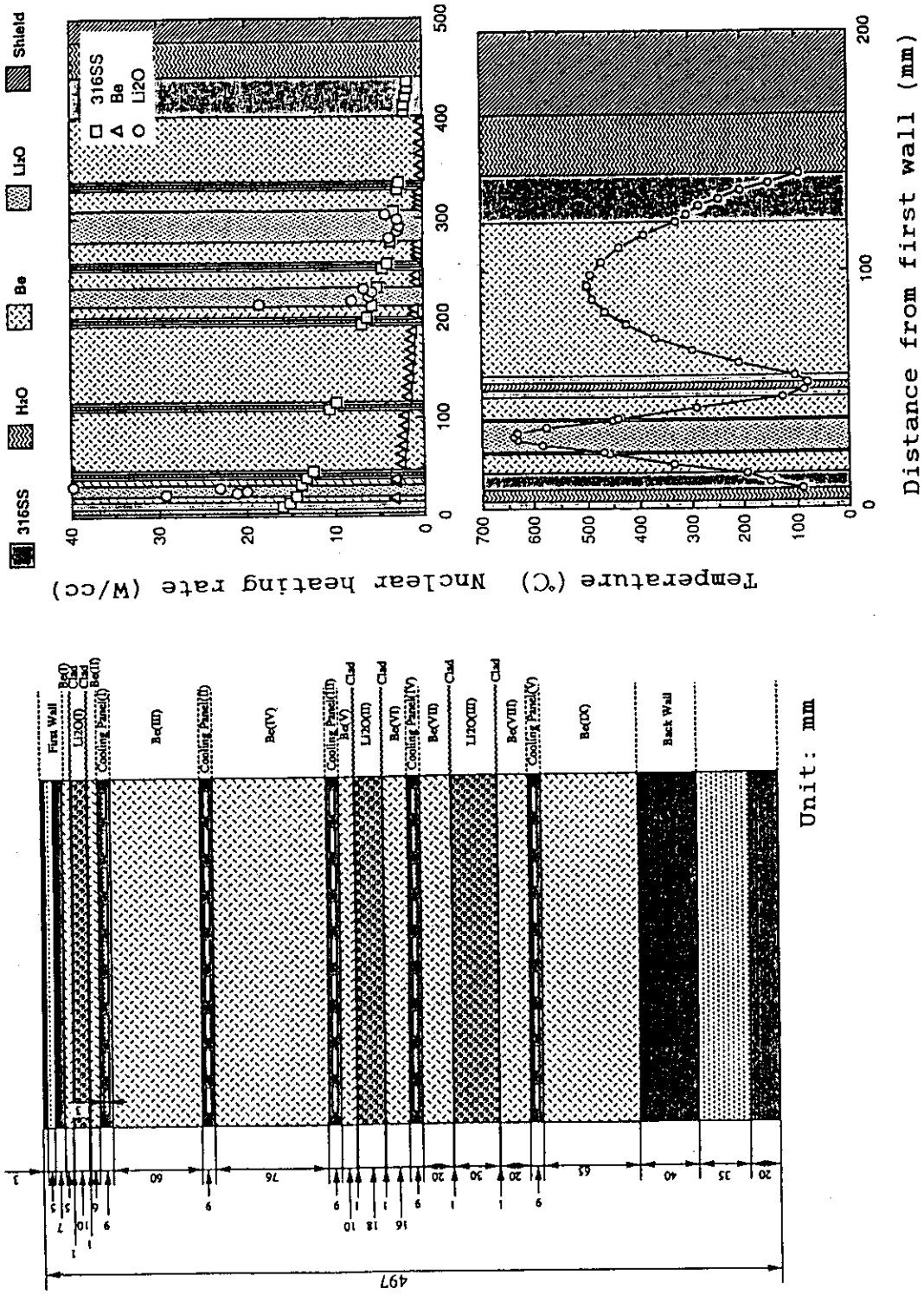

Fig. 1 Internal configuration, nuclear heating rate distribution, and temperature profiles of ITER blanket proposed by Japan

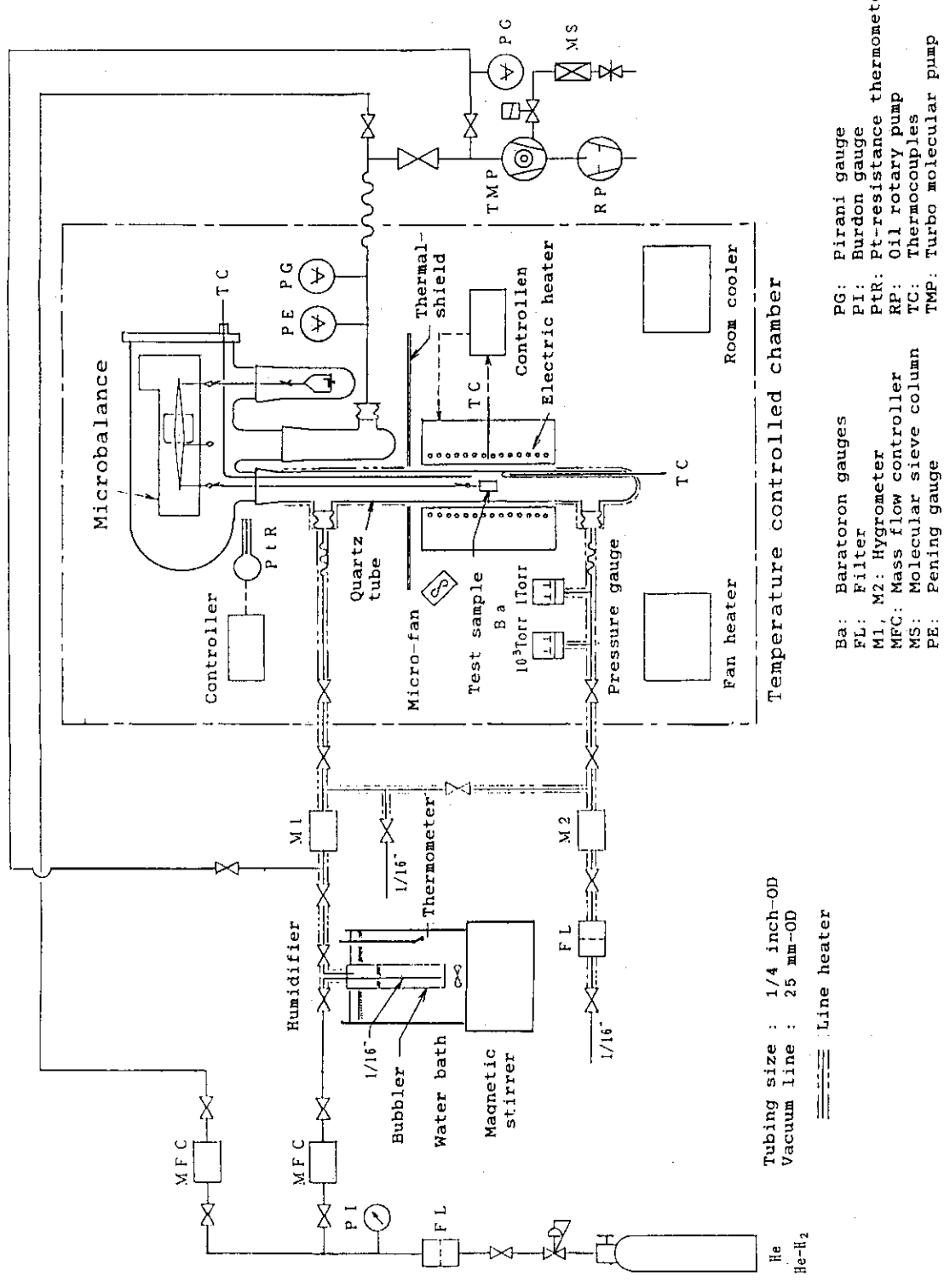

Fig. 2 Experimental apparatus flowsheet

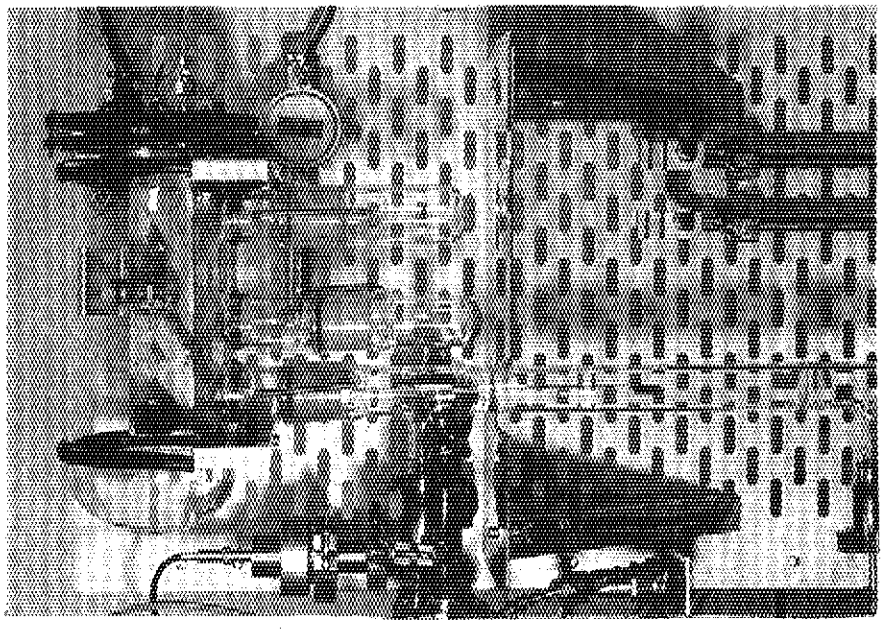

(b) Microbalance without furnace

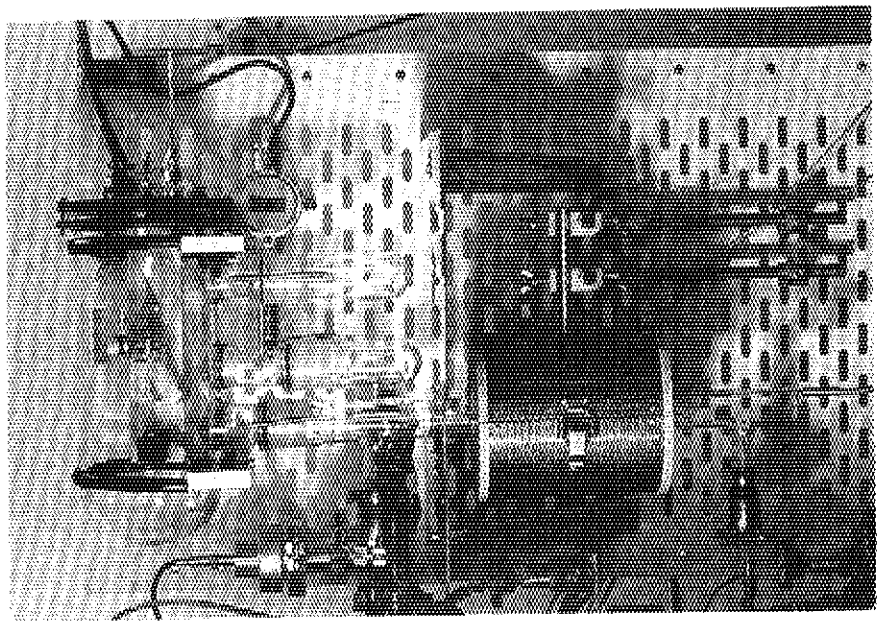

(a) Microbalance with furnace

Fig. 3 Setup of microbalance (CAHN-C2000)

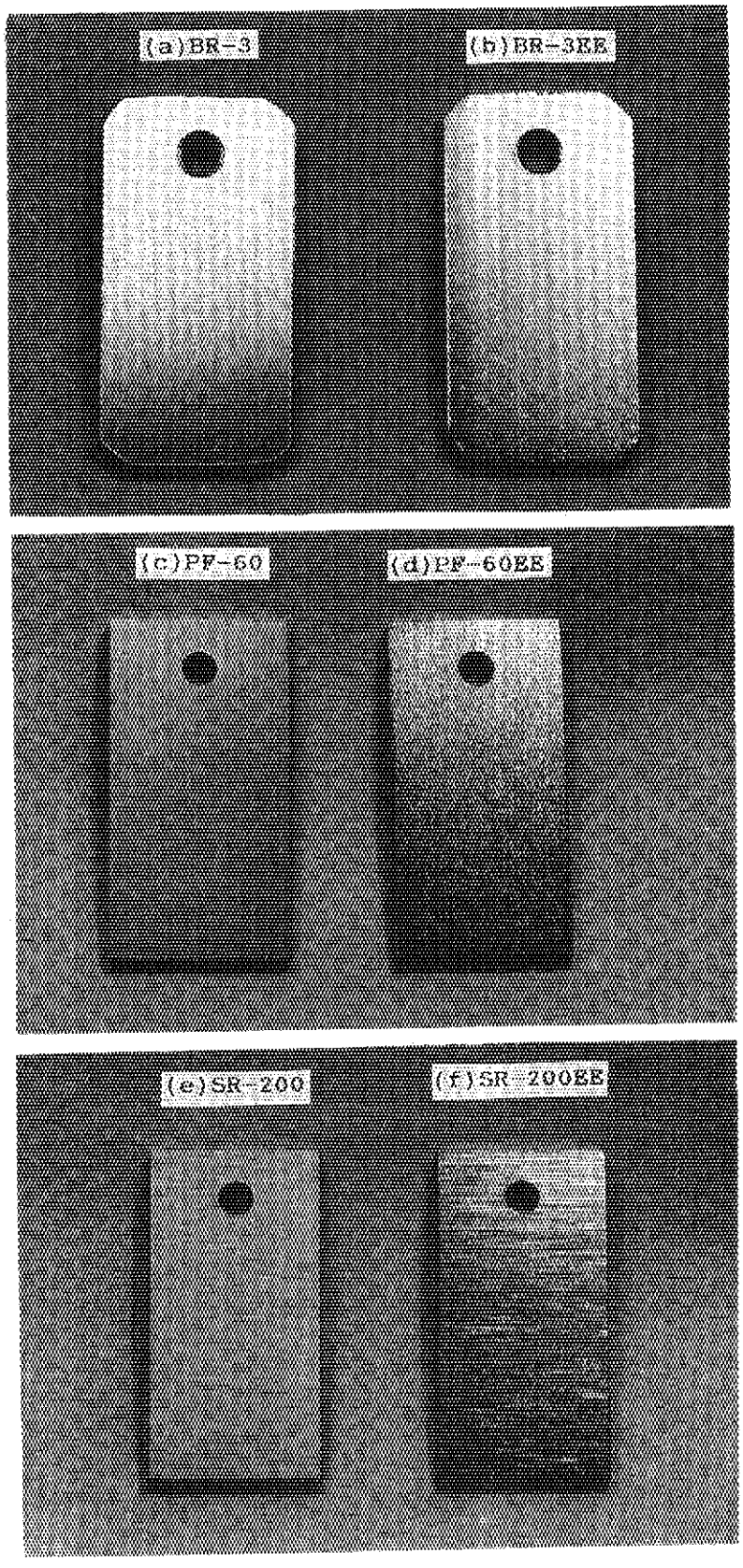

Fig. 4 Appearance of test samples
(a,c,e): mechanically ground
(b,d,f): chemically polished

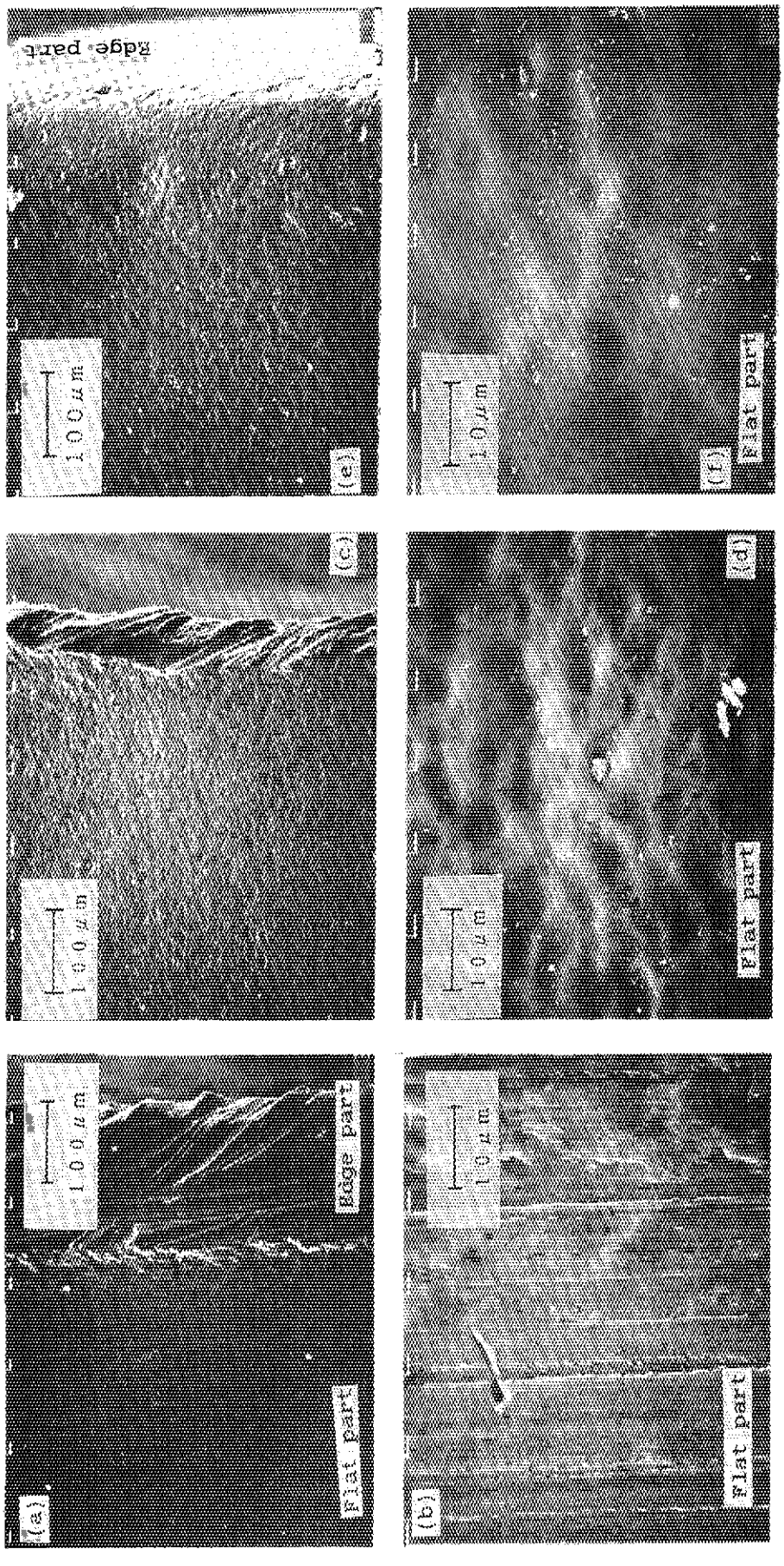

Fig. 5 Surface characteristics of BR-3 type before exposure test
(a),(b) BR-3 : mechanically ground
(c),(d) BR-3E : chemically polished (flat part)
mechanically ground (edge part)
(e),(f) BR-3EE: chemically polished (entire surface)

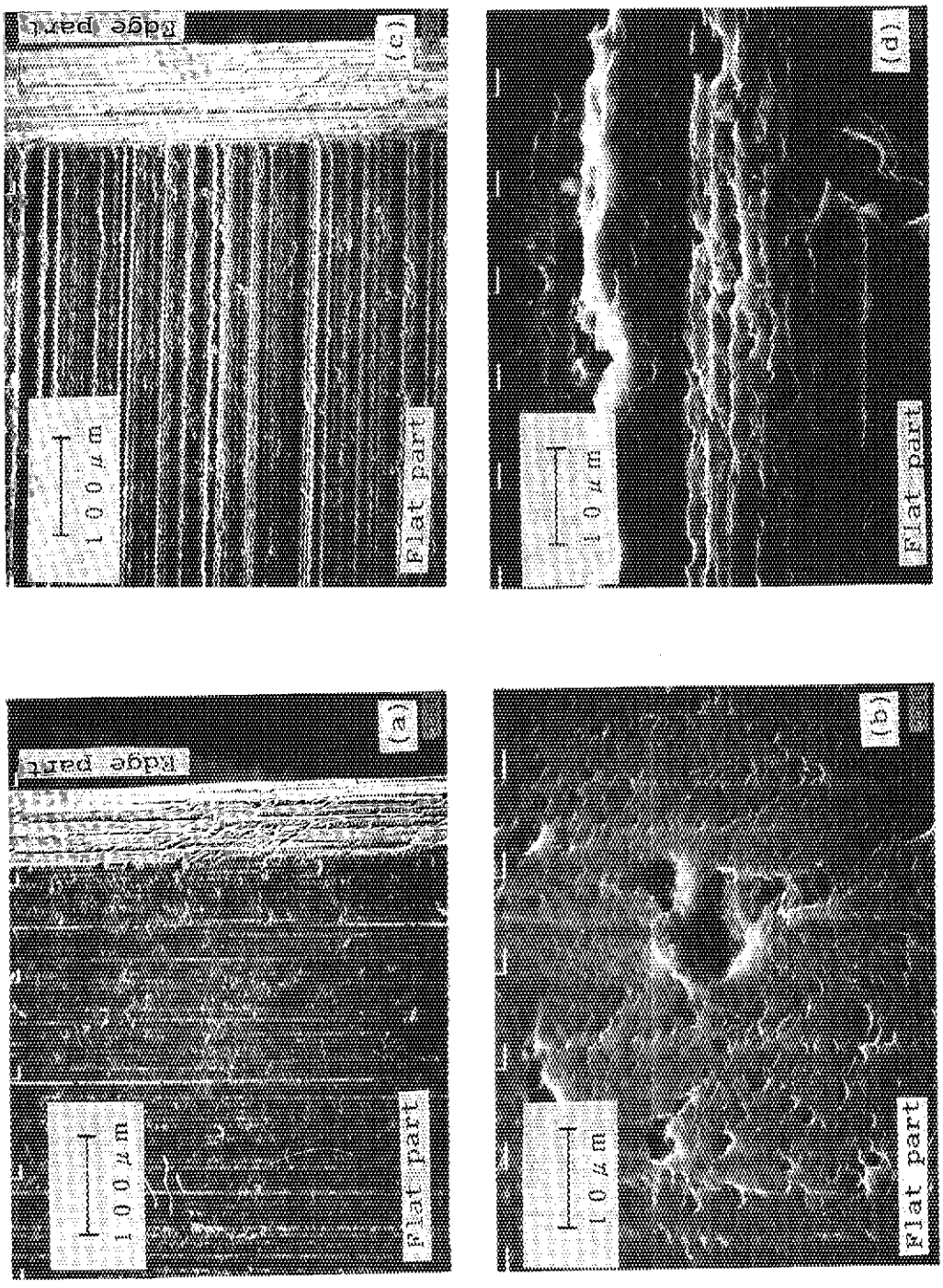

Fig. 6 Surface characteristics of PF-60 and SR-200
(a),(b) PF-60 : mechanically ground
(c),(d) SR-200: mechanically ground

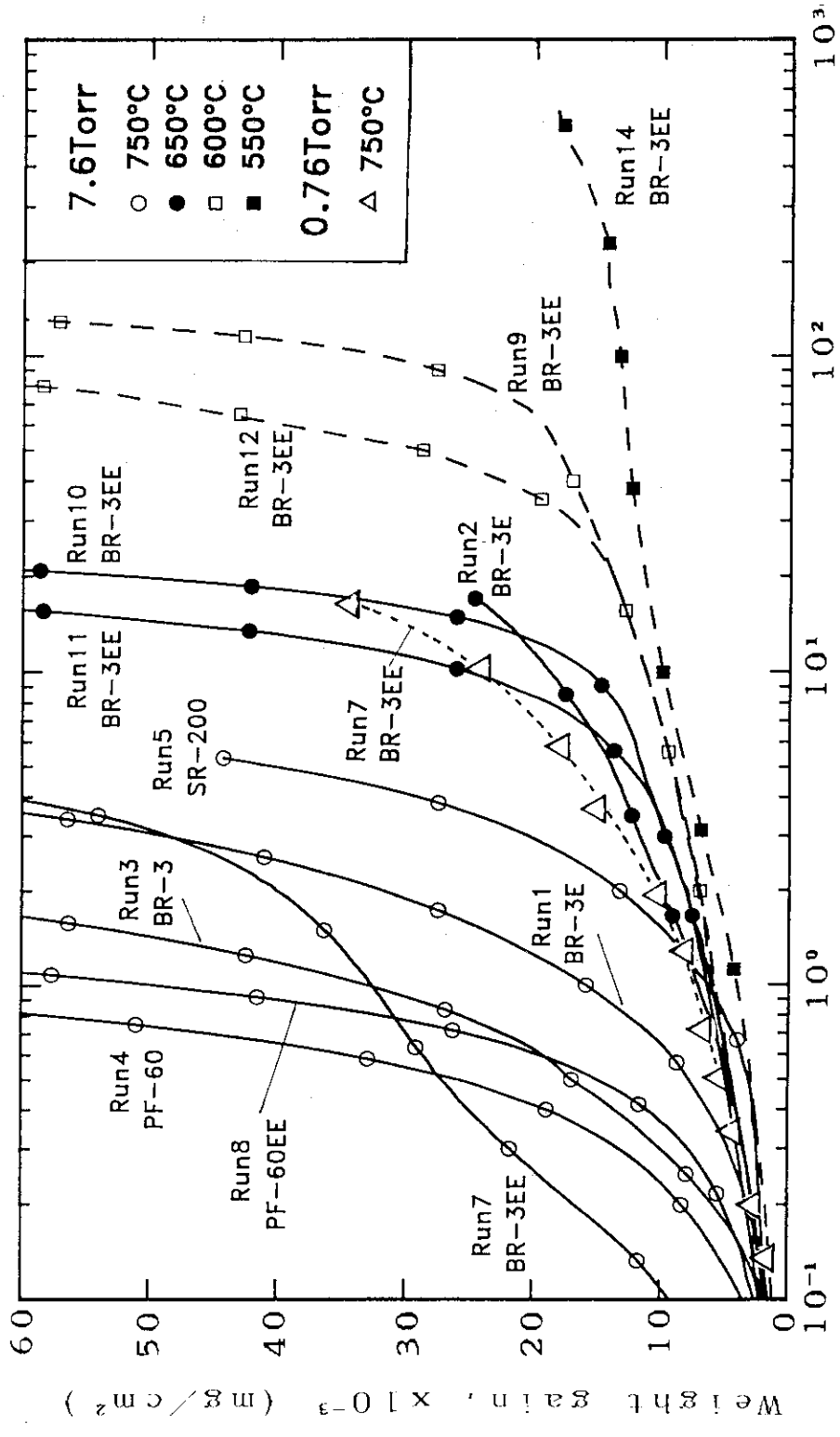

Fig. 7 Time depemdence of weight gain during exposure to water vapor

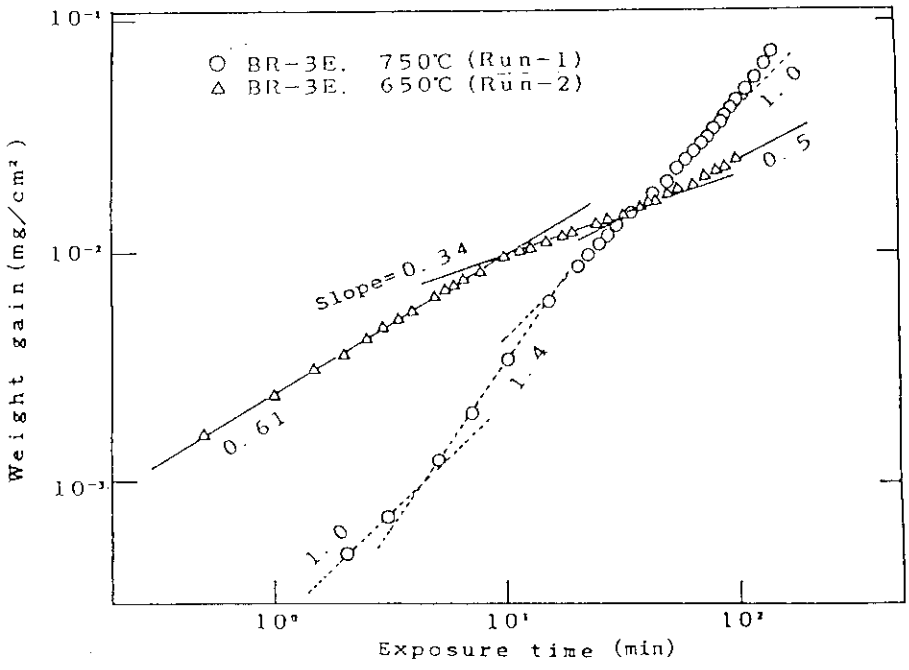

Fig. 8 Kinetic characteristics of derivative period of breakaway reaction at high vapor pressure of 7.6 Torr

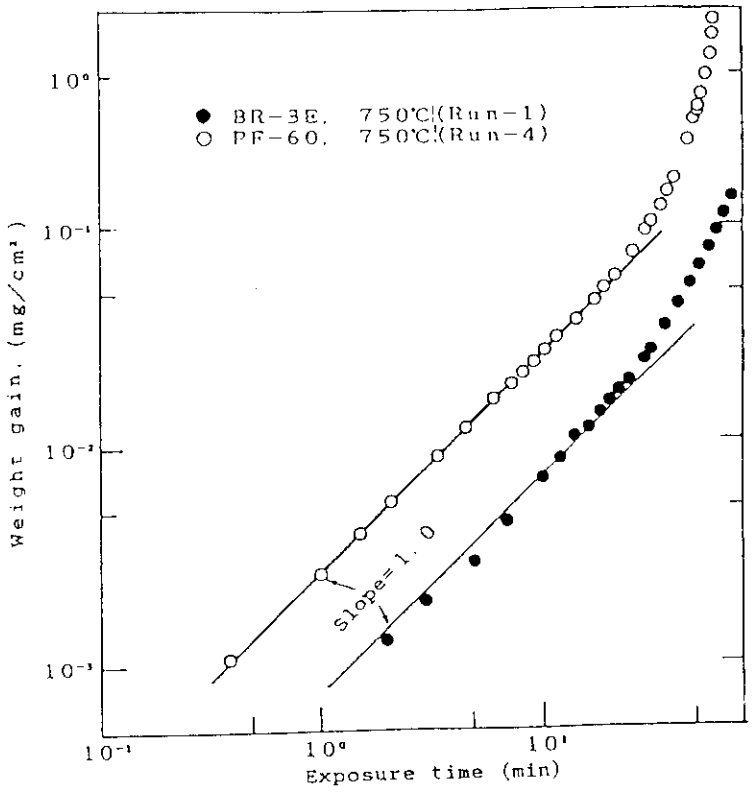

Fig. 9 Examples of linear reaction, which dominated derivative period for breakaway reaction

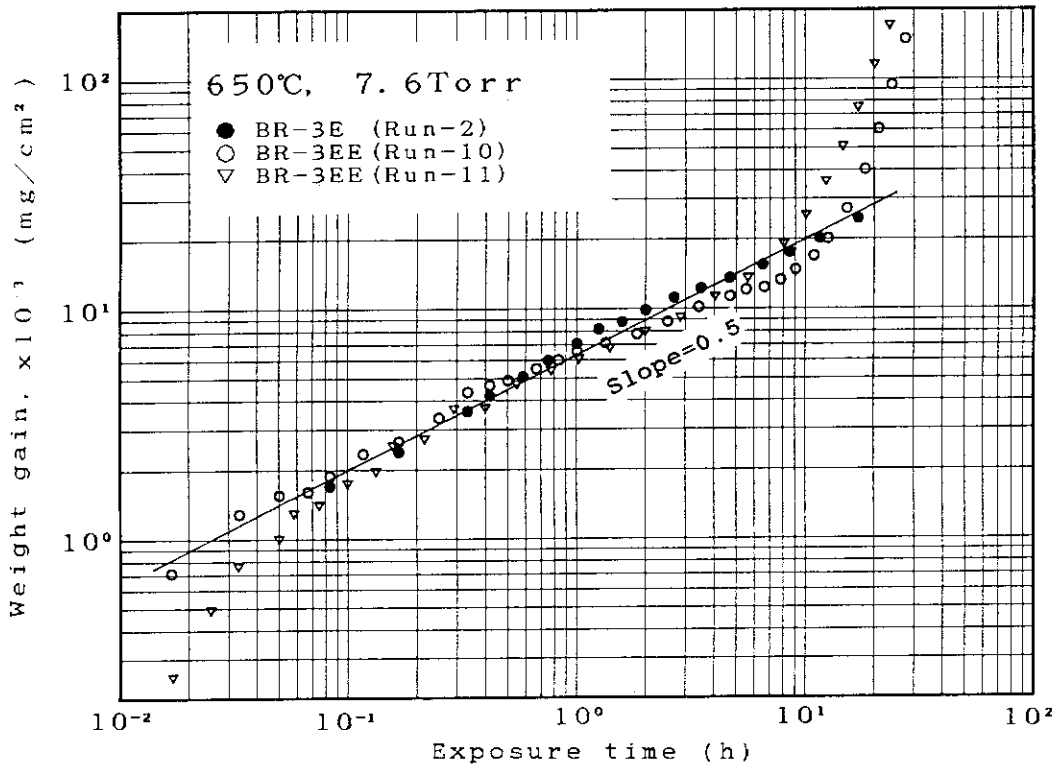

Fig. 10 Examples of parabolic reaction, which dominated derivative period for breakaway reaction

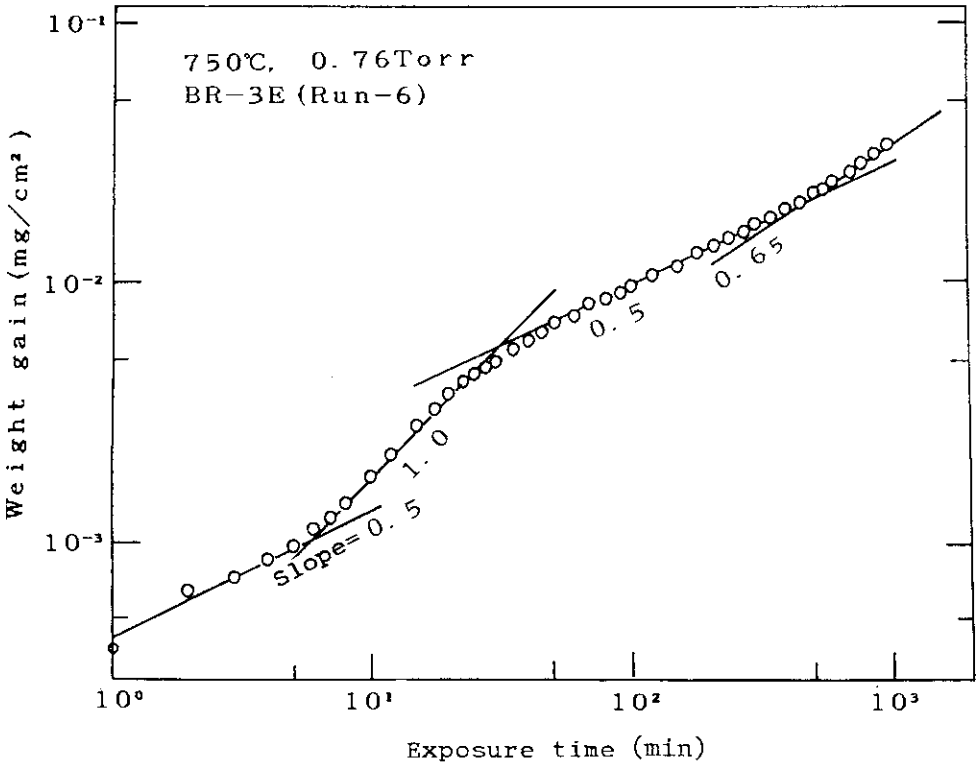

Fig. 11 Kinetic characteristics of derivative period of breakaway reaction at low vapor pressure

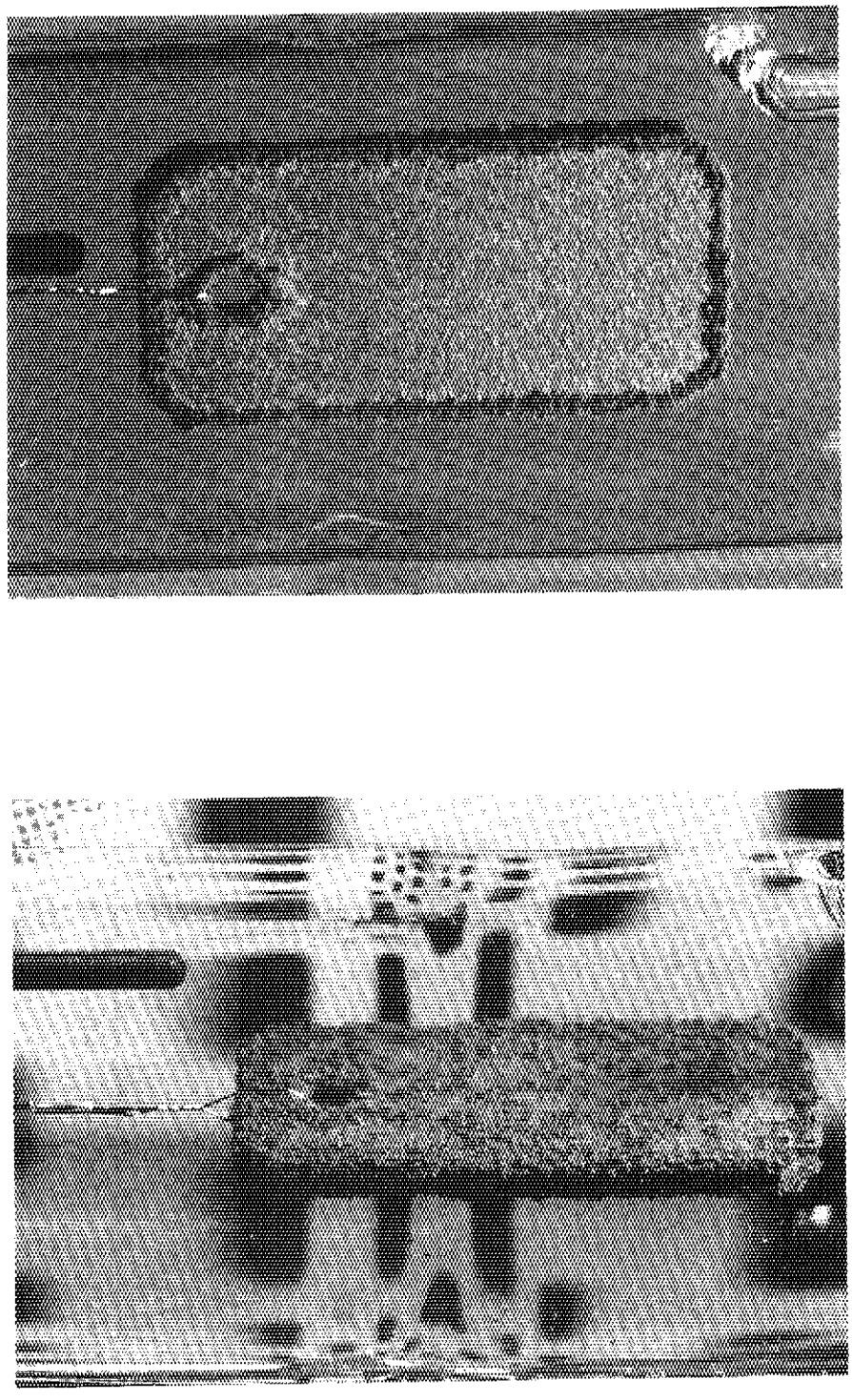

Fig. 12 Macroscopic appearance of test sample after breakaway reaction
(Run-1: BR-3, 750 °C, 7.6 Torr, 9.9 h)

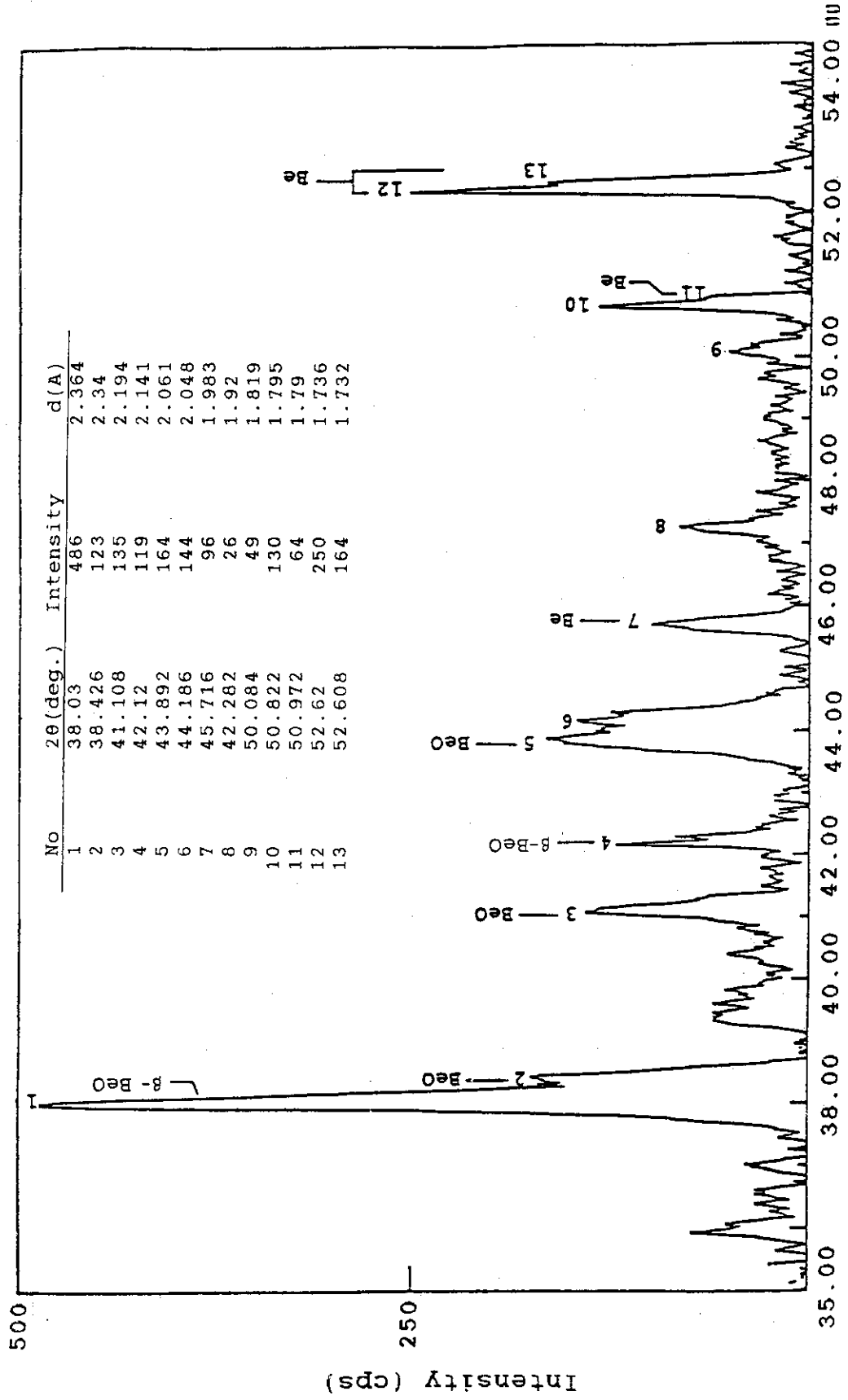

No	2θ(deg.)	Intensity	d(A)
1	38.03	486	2.364
2	38.426	123	2.34
3	41.108	135	2.194
4	42.12	119	2.141
5	43.892	164	2.061
6	44.186	144	2.048
7	45.716	96	1.983
8	42.282	26	1.92
9	50.084	49	1.819
10	50.822	130	1.795
11	50.972	64	1.79
12	52.62	250	1.736
13	52.608	164	1.732

Fig. 13 X-ray diffraction pattern of reaction product removed from surface of sample received break away reaction (Run-1: BR-3, 750 °C, 7.6 Torr, 9.9 h)

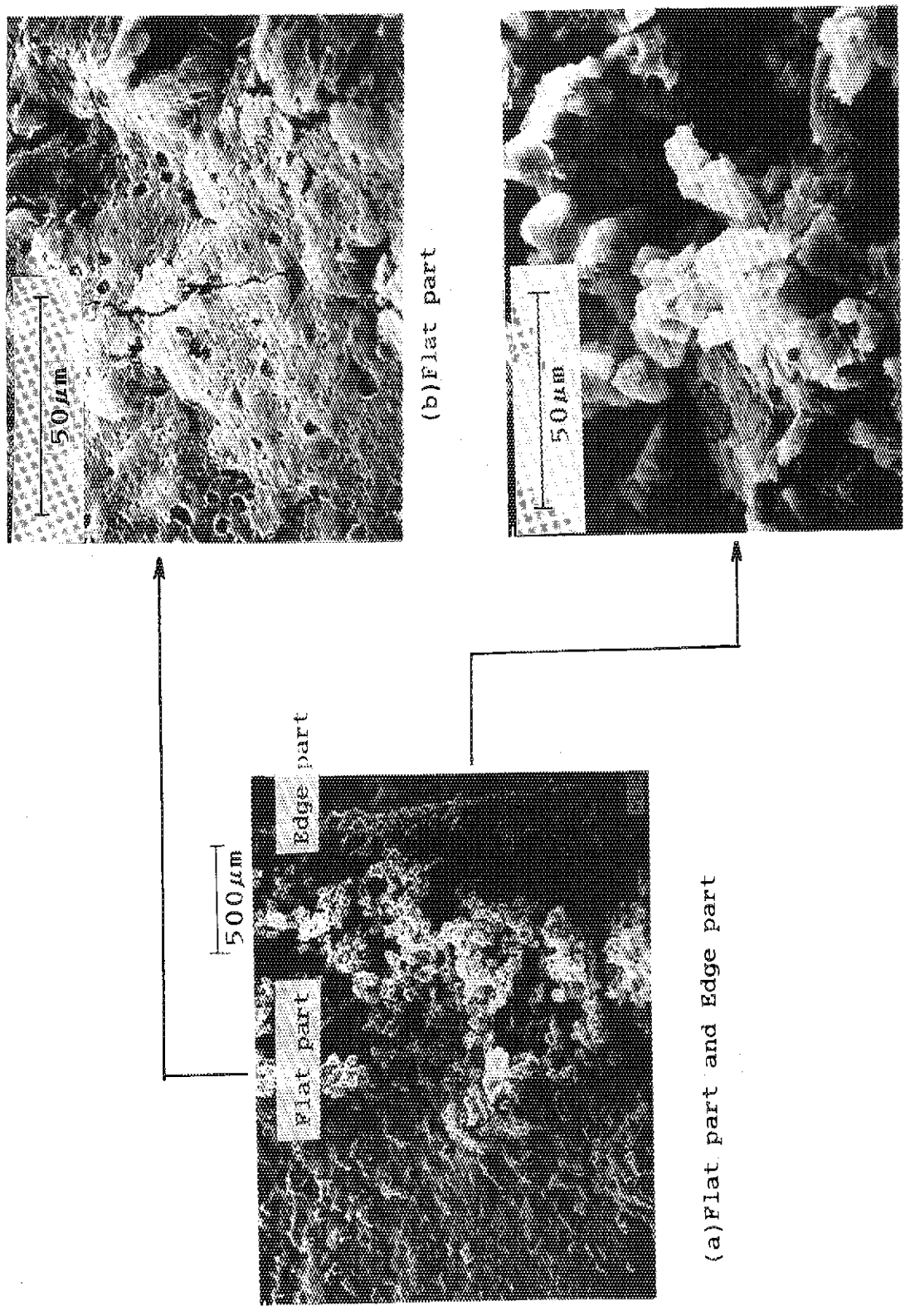

Fig. 14 Microscopic surface structure after breakaway reaction (Run-1: BR-3, 750 °C, 7.6 Torr, 9.9 h)

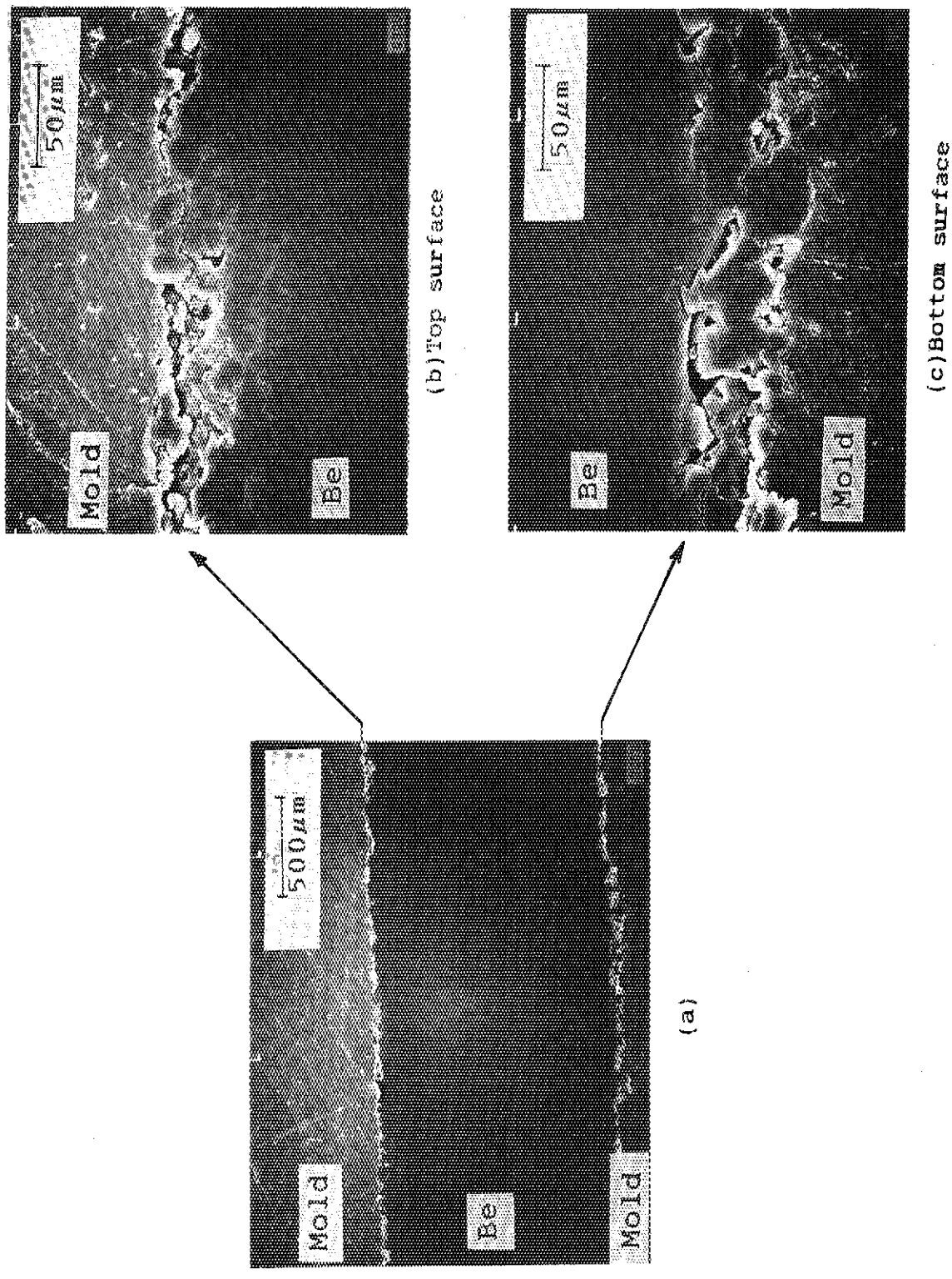

Fig. 15 Cross-sectional structure of reaction zones after breakaway reaction (Run-1: BR-3, 750 °C, 7.6 Torr 9.9 h)

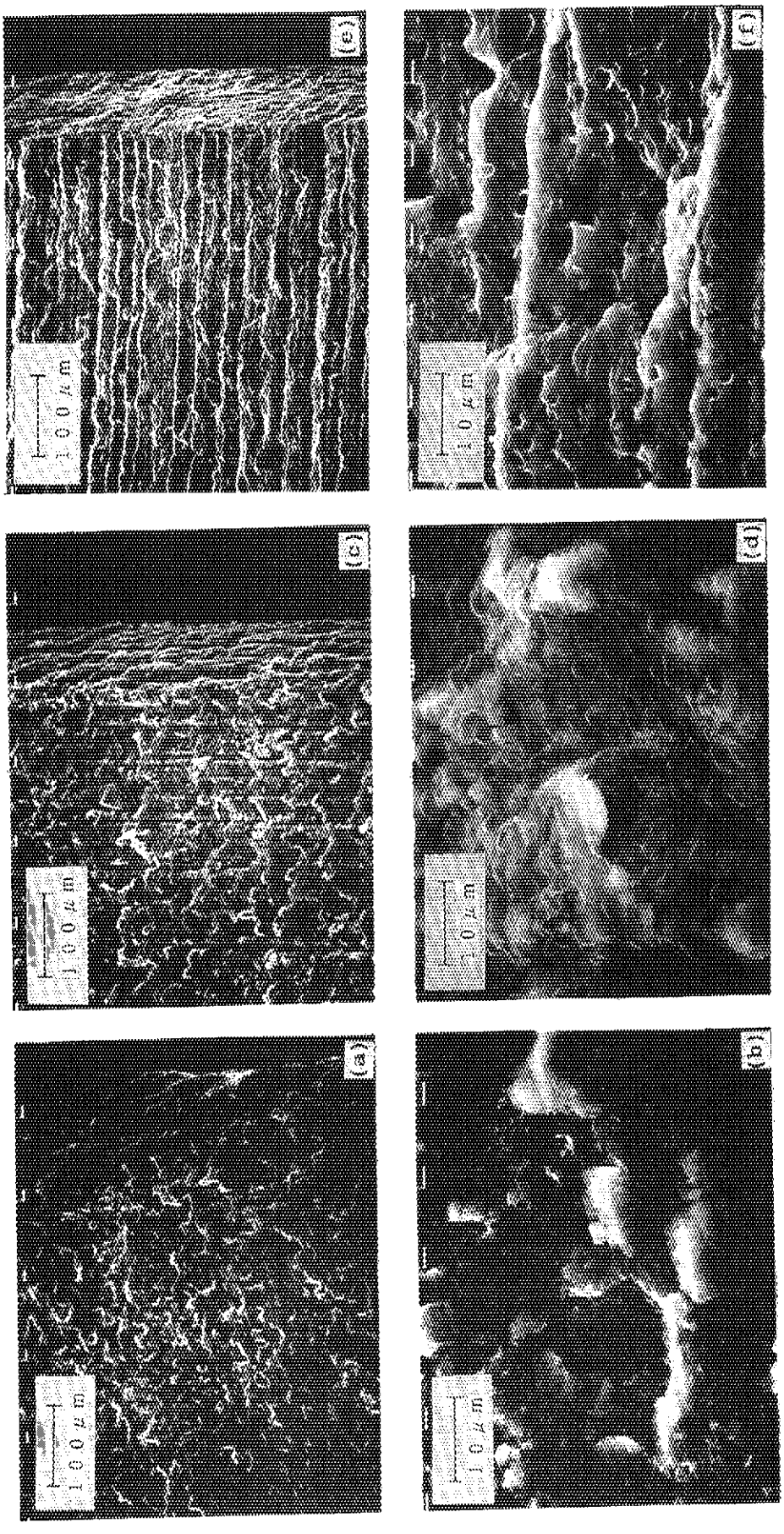

Fig. 16 Material comparison of surface microstructure after breakaway reaction at 750 °C and 7.6 Torr (Run-3: BR-3, Run-4: PF-60, Run-5: SR-200)

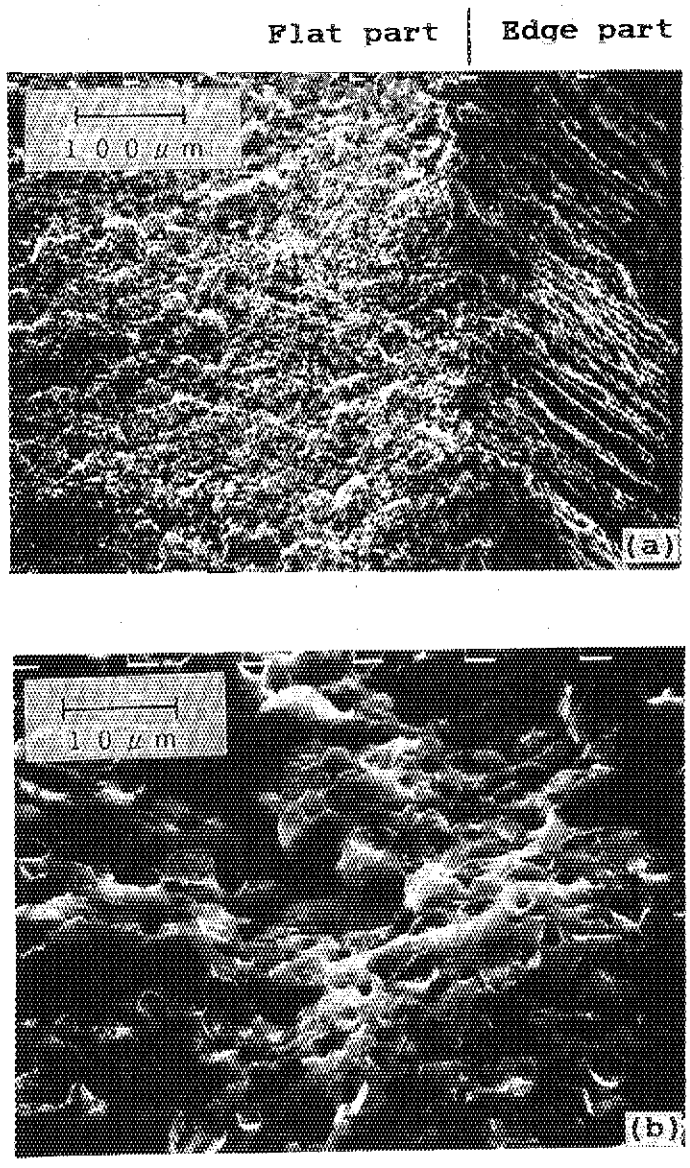

Fig. 17 Surface microstructure after breakaway reaction for low vapor pressure
(Run-6: BR-3E, 0.76 Torr, 750 °C)

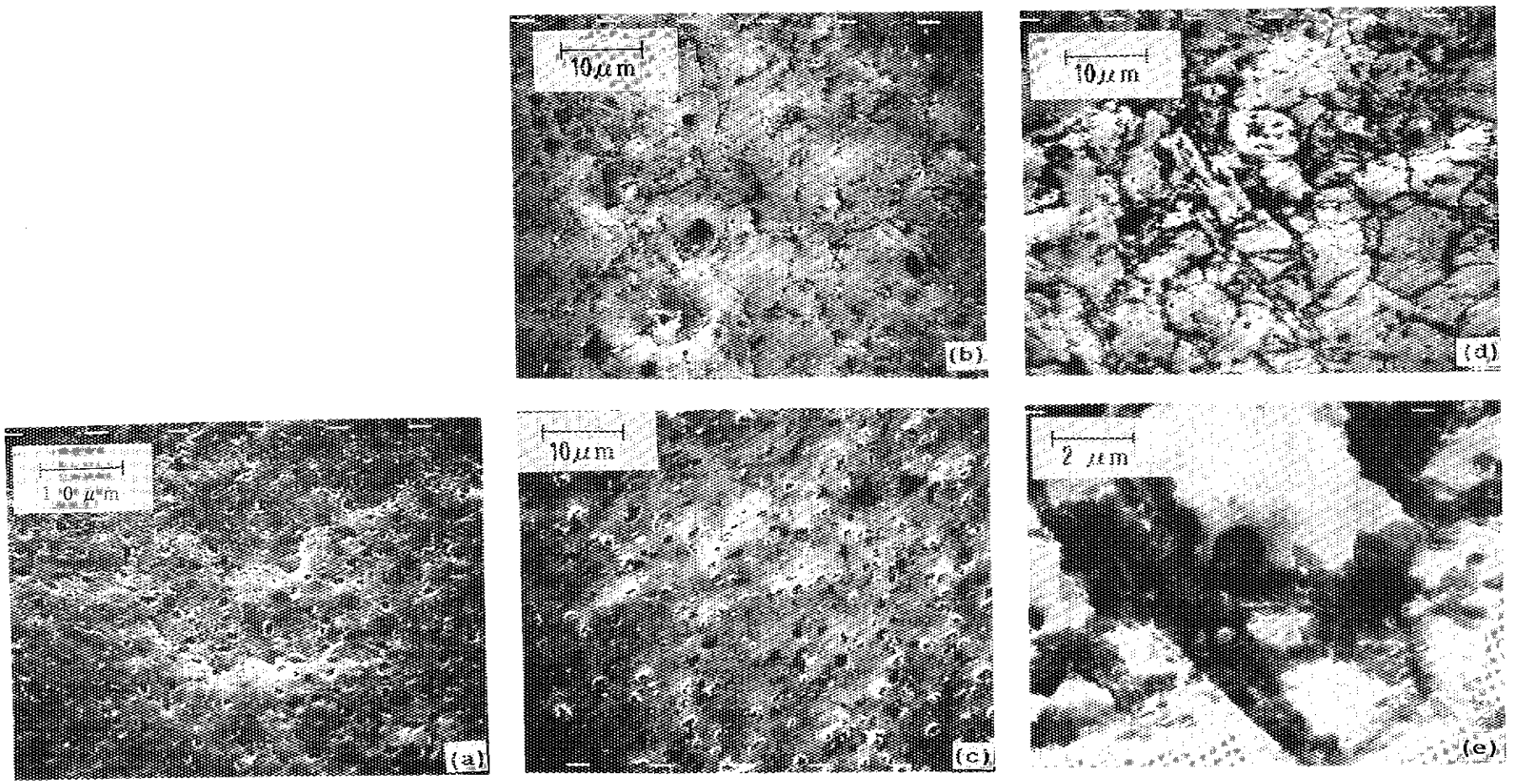

Run-2: (a)

Run-14: (b)-(e)

Fig. 18 Surface microstructure exposed at different temperatures with vapor pressure of 7.6 Torr (Run-2: BR-3E, 650 °C, 17 h, Run-14: BR-3EE, 550 °C, 600 h)

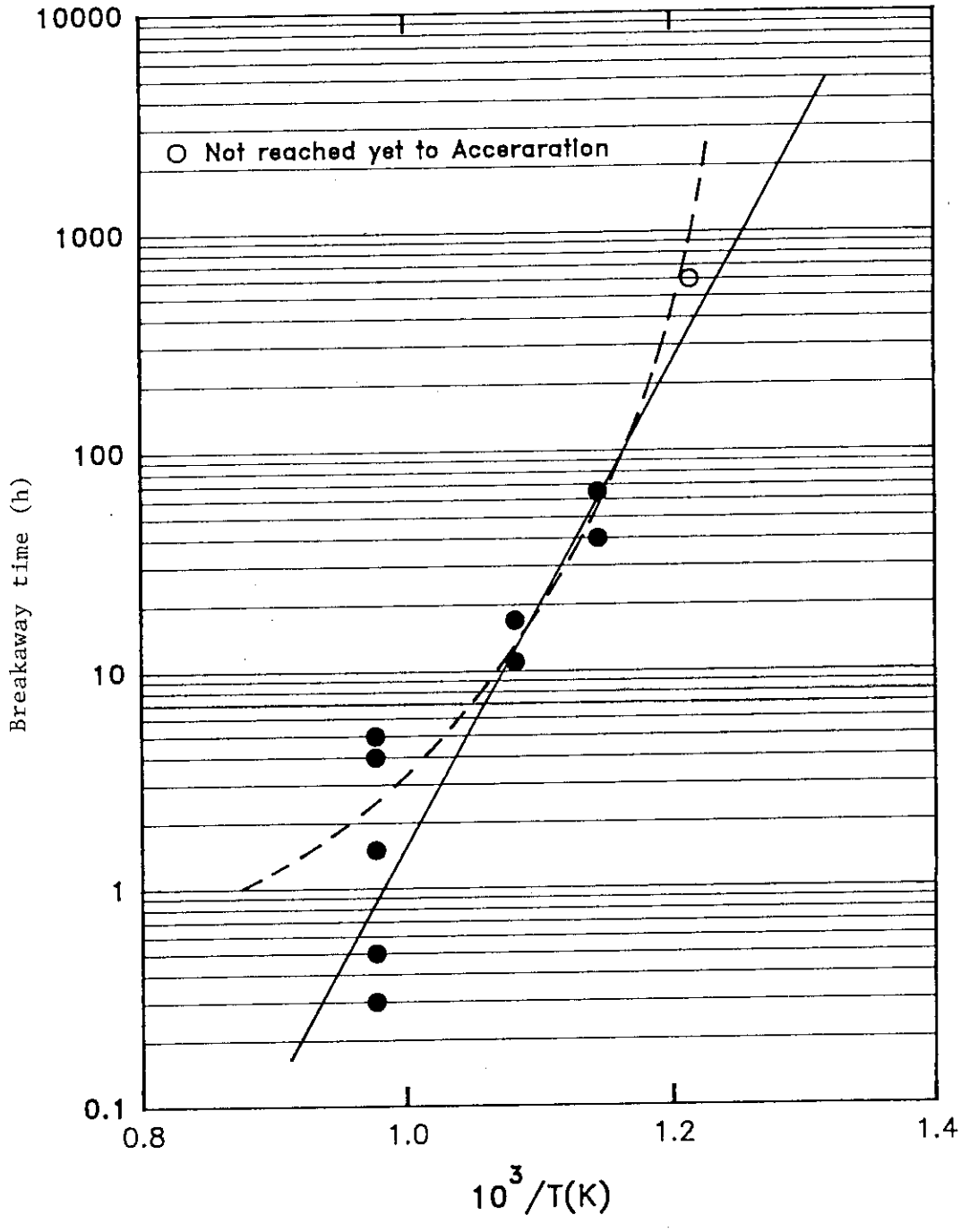

Fig. 19 Correlation of breakaway time and temperature